DOI: 10.17323/2587-814X.2022.4.19.35

Simulation of rates of traffic accidents involving unmanned ground vehicles within a transportation system for the 'smart city'

Andranik S. Akopov
E-mail: akopovas@umail.ru

Levon A. Beklaryan
E-mail: beklar@cemi.rssi.ru

Central Economics and Mathematics Institute, Russian Academy of Sciences
Address: 47, Nakhimovsky prospect, Moscow 117418, Russia

Abstract

This article presents an approach to simulation of the rates of road traffic accidents involving unmanned ground vehicles within a multi-agent intelligent transportation system for the 'smart city.' A new simulation model of an intelligent transport system has been developed which makes it possible to significantly reduce the number of potential road traffic accidents (TAs) and implements the concept of socially-centered management of the urban economy. The software implementation of such a large-scale agent-based model was carried out using the FLAME GPU framework, which allows us to effectively parallelize the agents' behaviour logic and consider their individual decision-making systems when modelling the spacial dynamics of an ensemble of unmanned ground vehicles (UGVs) interacting with other road users: the usual manned ground vehicles (MGVs), unexpected obstacles (e.g., pedestrians, etc.). Various scenarios of such agents' behaviour in an intelligent transportation system are studied, including the occurrence of an accident under certain conditions (e.g., under the high speed and traffic intensity of UGVs, etc.) and various configurations of the digital road network (DRN). We determine the parameter values that provide for the individual decision-making system of UGVs remaining stable with respect to the characteristics of the external environment (including in extreme situations), ensuring the safety of other road users on the scale of the 'smart city.'

Keywords: socially-centered urban management, agent-based modeling, intelligent transportation systems, smart city, simulation of traffic accidents, unmanned vehicles, FLAME GPU

Citation: Akopov A.S., Beklaryan L.A. (2022) Simulation of rates of traffic accidents involving unmanned ground vehicles within a transportation system for the 'smart city'. *Business Informatics*, vol. 16, no. 4, pp. 19–35. DOI: 10.17323/2587-814X.2022.4.19.35

Introduction

Nowadays, the transition to socially-centered management of the urban economy within the development of the 'smart city' [1] is being updated as a complex urban ecosystem that combines a number of interrelated subsystems. Among them, one can highlight intelligent transportation systems as the most important factor providing a safe and comfortable state of the urban population. The importance of rational management for the 'smart city' system is due to the need to transform the urban environment in a direction that ensures a fundamental improvement in road traffic safety. Thus, for instance, the present level of traffic congestion in the Moscow agglomeration, according to various expert estimates, is from 60 to 70% and continues to grow annually (due to an increase in the number of personal vehicles, deficiencies in the characteristics of existing road networks and other factors). The degeneration of the road situation leads to many negative consequences: the occurrence of road traffic accidents (TAs), an increase in the time and cost of delivering marketable products, faster wear of the road surface, environmental degradation and other negative social consequences. Therefore, it is necessary to develop an intelligent information-analytical system for urban economy management which provides the possibility of introducing ground unmanned vehicles (UGVs)[1] and related transportation infrastructure. A clear advantage of the UGV is the ability to organize effective 'car sharing,' i.e. the shared use of unmanned vehicles by many people. The number of required UGVs in such shared use may be relatively small, and the level of security under certain conditions is quite high. In the future, this will make it possible to significantly reduce the number of vehicles on roads and improve the quality of the urban environment. At the same time, we know that accidents regularly occur in Moscow and other large metropolitan areas, including those involving UGVs. Such situations are a significant barrier to the wide dissemination and introduction of UGVs in the urban environment, since, in addition to the high cost of damage from road accidents, there are risks to life and health for all road users.

Previously, in [2–4], the existence of scenarios for accident-free movement of the UGVs ensemble interacting with manned ground vehicles (MGVs) has been shown for various configurations of the digital road networks and other environment characteristics. In particular, in the work [2] general conditions leading to occurrence of such accidents (mainly vehicle manoeuvres in dense traffic conditions) have been determined with the use of the developed agent-based model [5, 6]. Thus, the 'turbulence' and 'crowding' effects arise with an increase in the density of UGVs and MGVs, when some drivers seek to increase their personal space through frequent lane changes, overtaking and braking. As a rule, this leads to an even greater slowdown in traffic, creating difficulties for other road users, their 'pushing out' from their original route, errors dur-

[1] https://www.m24.ru/news/proisshestviya/27042021/163077

ing forced manoeuvres and the occurrence of an accident [7–9]. At the same time, of greatest interest are the particular conditions for the occurrence of accidents involving various agents: UGVs, MGVs, MGVs with anomalous behavior, pedestrians, cyclists, etc., as well as the possibility of developing an individual decision-making system for UGVs that is as stable regarding the environment characteristics. Such the system can be based on modeling and solving emerging problem situations [10, 11], using fuzzy rules in manoeuvres [2] and a phenomenological approach to control of the radius of an agent-UGV's personal space in manoeuvres and unexpected appearance of pedestrian-obstacles [4]. Moreover, it can use optimal routing for UGVs that allows them to avoid possible undesirable interactions with other road users [12–16].

Note that previously the phenomenological approach was proposed for modeling crowd behavior [17], considering the influence of the 'crowd effect' and other environmental characteristics (in particular, its configuration). A multi-agent system for control of UGVs has been developed based on this approach [5, 6]. For this purpose, the large-scale agent-based simulation framework FLAME GPU was used[2] [5, 18, 19]; it makes it possible to efficiently parallelize the logic of agents' behavior and consider their individual decision-making systems when modeling the spacial dynamics of an ensemble of interacting vehicles. On the other hand, the phenomenological approach is based on Dirk Helbing's studies [20, 21], which deal with models of humans and pedestrians' behavior under the influence of social forces.

Within the concept of the 'smart city' development, control systems for unmanned railway vehicles [22, 23] are also of great interest: they can be used to form optimal routs for freight wagons (controlled by unmanned locomotives) for a given set of freight wagons and a list of requests for a cargo transportation. Also, a promising area of research is the use of fuzzy [4, 5] and hierarchical clustering [24] methods to identify problem areas of the urban road network [25] (e.g., traffic jams, accident locations, etc.).

This paper proposes an approach to modeling the rates of accidents and improving road safety within the scale of the 'smart city' by combining computational and expert decision-making methods. A similar approach is also used in strategic management systems [26, 27], and its advantage is the ability to evaluate and generalize trade-offs by experts, obtained, in particular, as a result of optimization experiments with the simulation model so developed. Such an expert assessment allows you to consider the off-model features of an intelligent transportation system, in particular, financial and technological restrictions that affect the possibility of reconfiguring street road networks, as well as legal requirements that can be applied to tasks of the 'smart city.'

The purpose of this article is to develop a new socially-centered approach to urban management based on modeling the dynamics of traffic accidents involving unmanned vehicles within a multi-agent intelligent transportation system of the 'smart city' and implementation on the FLAME GPU framework, as well as determining the conditions under which the UGV's individual decision-making system keeps up resilience to risk factors to ensure the safety of other road users. An information-analytical system for the rational management of the urban economy can be developed based on the proposed model. Furthermore, some recommendations are formulated to increase the transformation of the urban environment (in particular, the transport infrastructure), which is one of the important areas of research in the field of business informatics.

[2] https://flamegpu.com/

1. Description of the model

Previously, an agent-based simulation model of the UGVs' behavior in an interaction with MGVs and other agents of the intelligent transportation system was developed [2, 3]. This model uses a system of finite-difference equations with a variable structure to implement various scenarios for vehicle communications with each other (V2V), with pedestrians (V2P), with the environment (V2I), etc. (*Fig. 1*). Such an approach allows you to consider multiple scenarios of UGVs interaction with other participants of the digital road network (DRN), for instance, MGVs, pedestrians, stationary obstacles, etc., which differ significantly in their velocities and sizes, and which directly affect the decision speed of UGVs.

At the same time, digital road networks such as 'roundabouts" [2] and the 'Manhattan grid' [3] with a limited set of possible configurations were considered. In this paper, we propose to significantly complicate the geometry of digital road networks, bringing it closer to the scale of the 'smart city,' as well as to develop an individual UGV's decision-making system that is as stable as possible regarding risk factors, such as the unexpected appearance of static obstacles, pedestrians, cyclists, etc. (*Fig. 2*).

Such stability is ensured by braking through increasing the radius of the vehicle's personal space (with a subsequent gradual decrease to a normal level) when obstacle objects appear that have different linear speeds, if the path length from the vehicle to the object is sufficient for braking (*Fig. 2a*), or manoeuvering

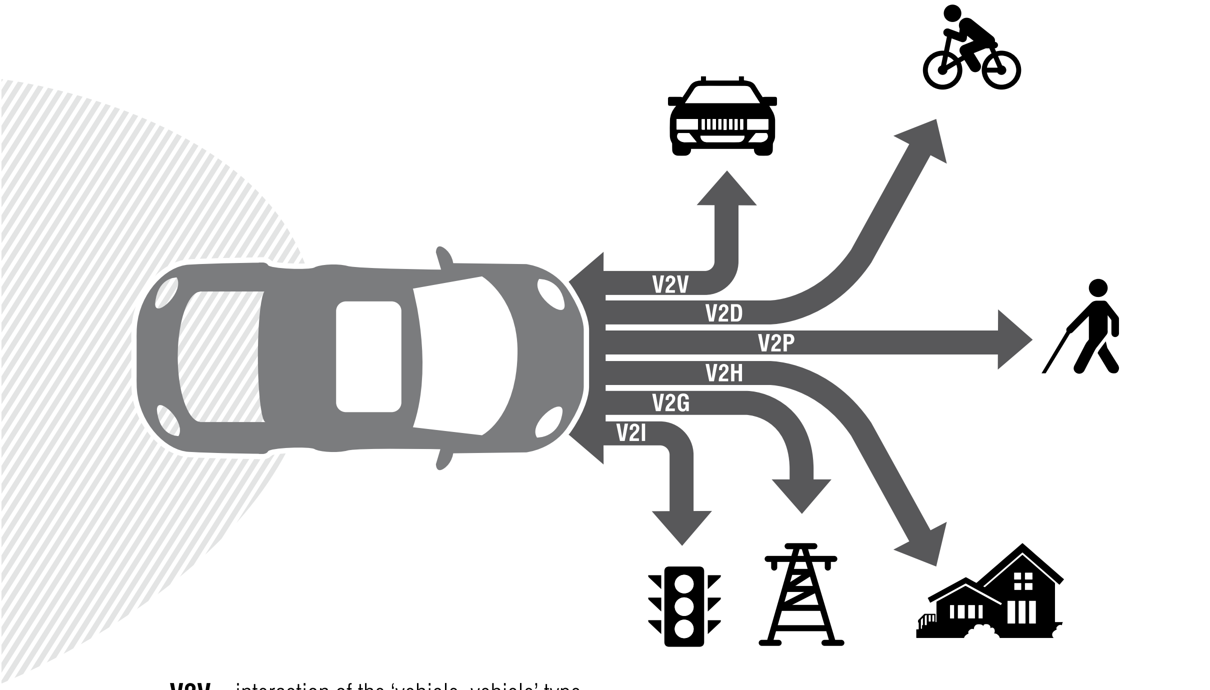

V2V – interaction of the 'vehicle–vehicle' type
V2D – interaction of the 'vehicle–device' type (i.e. a moving object)
V2P – interaction of the 'vehicle–pedestrian' type
V2H – interaction of the 'vehicle–home' type (i.e. a stationary object)
V2G – interaction of the 'vehicle–grid' type (i.e. a charging station)
V2I – interaction of the 'vehicle–infrastructure' type (i.e. a smart traffic light)

Fig. 1. Illustration of the interaction of a vehicle (V) with various agents of an intelligent transportation system.

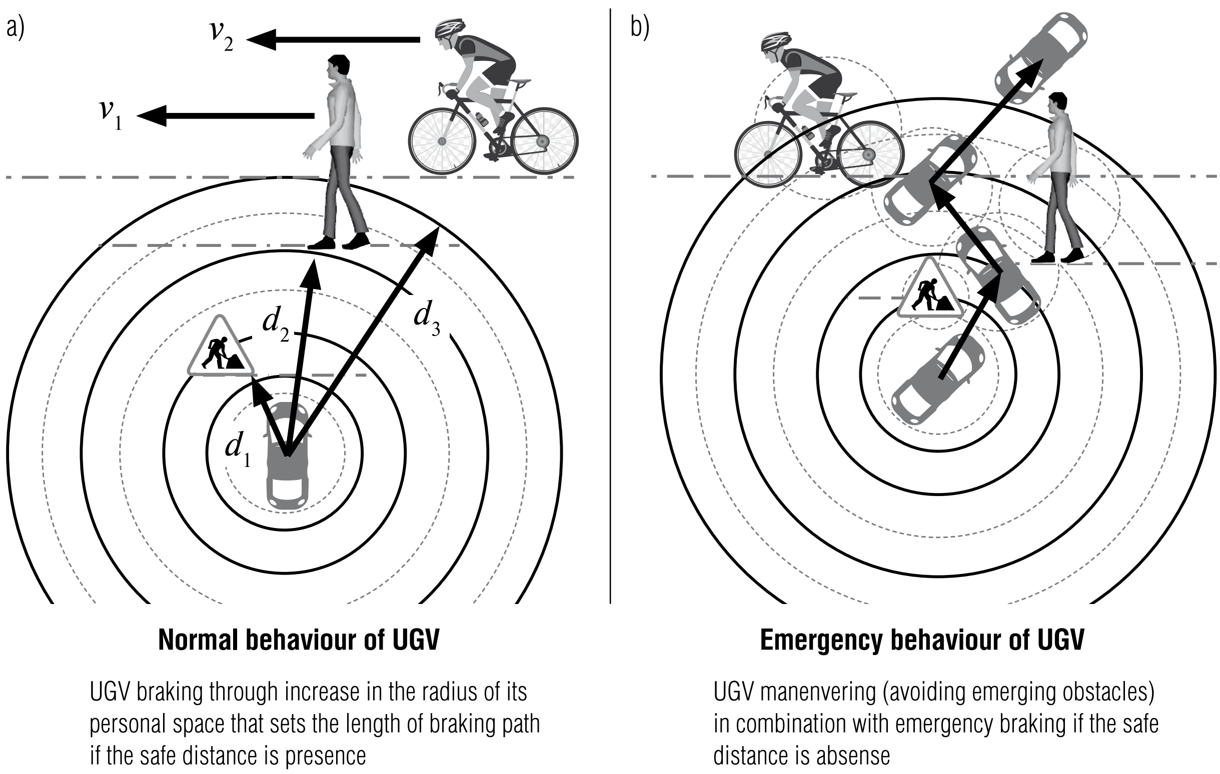

Fig. 2. Illustration of the process of interaction between the vehicle and other agents of the intelligent transportation system:
a) if the safe distance between the vehicle and obstacle is maintained;
b) if the path length is insufficient for emergency braking.

so as to bypass emerging obstacles within its lane in combination with emergency braking (*Fig. 2b*) in the case when the distance between the vehicle and the obstacle that has arisen does not allow avoiding a collision through braking.

If a stationary obstacle (e.g., a road works sign) suddenly appears in front of a vehicle moving at an average speed of 60 km/h, then the decision speed is quite high to avoid an accident by minimally increasing the radius of the vehicle's personal space up to the level d_1 (approximately 20 m in a dry, 30 m in wet and 60 m in icy road surfaces, respectively) if a pedestrian suddenly appears (at an average speed v_1 = 4–7 km/h), then in order to avoid an accident with the UGV, it is necessary to increase the radius of personal space to the level d_2 (approximately 30 m in dry pavement, 50 m in wet and 70 m in icy), and finally, if a fast moving cyclist unexpectedly appears (at an average speed v_2 = 10–15 km/h), then the radius of the personal space of the UGV should be increased to the level d_3(approximately 40 m in dry pavement, 60 m in wet and 80 m in icy). The increase in the radius of the UGV's personal space is caused by decrease in the reaction speed in appearance of a moving obstacle and increase in the UGV's time spent to correctly recognize the corresponding event.

At the same time, various configurations (schemes) of the street road network are possible [25], among which the radial-circular one should be singled out as an example (*Fig. 3*). It should be noted that there are possible configurations of the street road network, for example, extended radial-ring, rectangular, rectangular-diagonal, rectangular-ring, etc.

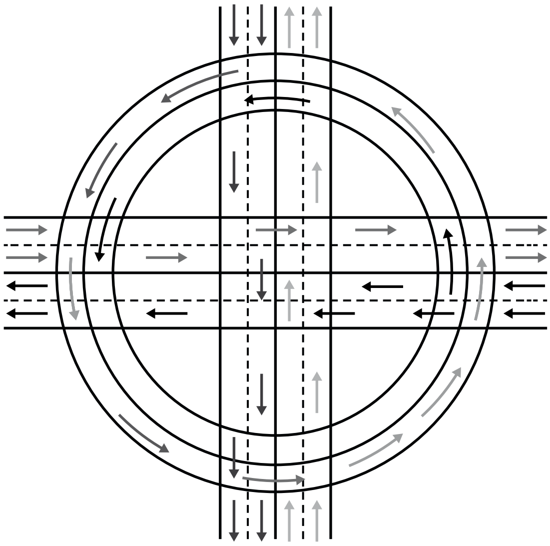

Fig. 3. A simple radial–ring scheme of the street road network.

The arrows in *Fig. 3* show the directions of traffic flows. In such a scheme, each vehicle entering the DRN and staying in decision zones (i.e. at intersections) has two alternative routes of movement (e.g., left-to-right or a detour) that ensure the implementation of outgoing traffic.

Next, an abstract description of the developed model of UGVs' behavior, the spacial dynamics of which correspond to the configuration of a simple radial-ring scheme of the street road network is given (*Fig. 3*).

Here,

- $T = \{t_0, t_1, ..., |T|\}$ is the set of time moments (by minutes),$|T|$ is the total number of time moments; $t_0 \in T$, $t_{|T|} \in T$ are the initial and final time moments;
- $I = \{ i_1, i_2, ..., i_{|I|}\}$ is the set of indices for unmanned ground vehicles (UGVs), where $|I|$ is the total number of UGVs;
- $B = \{1, 2, ..., |B|\}$ is the set of indices of obstacle types:$b = 1$ is an agent-MGV, $b = 2$ is a stationary obstacle (e.g., sign of road works, pit, etc.), $b = 3$ is a pedestrian, $b = 4$ is a cyclist, etc.), which may suddenly appear on the road, where $|B|$ is the total number of types of possible obstacles;
- $J_b = \{j_{b1}, j_{b2}, ..., j_{|Jb|}\}$, $b \in B$ is the set of indices of agent-obstacles belong to the b-type, where $|J_b|$ is the total number of agent-obstacles;
- $U = \{ u_1, u_2, ..., u_{|U|}\}$ is the set of indices of the DRN's characteristics that significantly affect the dynamics and manoeuverability of the agent-UGVs, in particular, the state of the road surface, the illumination level, etc., where $|U|$ is the total number of the DRN's characteristics.

Then, the density of the vehicilar flow around some $\tilde{i}^{th}$-agent-UGV ($\tilde{i} \in I$) at moment t_{k-1} ($t_{k-1} \in T$) is equal to

$$\rho_{\tilde{i}}(t_{k-1}) = \sum_{i=1}^{|I|} m_{\tilde{i}i}(t_{k-1}) + \sum_{b=1}^{|B|} \sum_{j_b=1}^{|J_b|} \tilde{m}_{\tilde{i}j_b}(t_{k-1}), \quad (1)$$

where

$$m_{\tilde{i}i}(t_{k-1}) = \begin{cases} 1, \text{ if } d_{\tilde{i}i}(t_{k-1}) \le R, \\ 0, \text{ if } d_{\tilde{i}i}(t_{k-1}) > R, \end{cases} \quad (2)$$

$$\tilde{m}_{\tilde{i}j_b}(t_{k-1}) = \begin{cases} 1, \text{ if } \tilde{d}_{\tilde{i}j_b}(t_{k-1}) \le R, \\ 0, \text{ if } \tilde{d}_{\tilde{i}j_b}(t_{k-1}) > R, \end{cases}$$

$$i \in I,\ b \in B,\ j_b \in J_b.$$

Here, $\{d_{\tilde{i}i}(t_{k-1}), \tilde{d}_{\tilde{i}j_b}(t_{k-1})\}$ is the Euclidean distance between the $\tilde{i}^{th}$-agent-UGV ($\tilde{i} \in \tilde{I}$) and each other i^{th}-agent-UGV ($i \in I$), as well as between the $\tilde{i}^{th}$-agent-UGV and j_b^{th}-agent-obstacle ($b \in B$, $j_b \in J_b$) at the moment t_{k-1} ($t_{k-1} \in T$), respectively, and the R is the fixed viewing radius chosen to estimate the density of vehicles.

The radius length of the agent-UGV's personal space depends on the density of the surrounding space, as well as on the distance to the agent-obstacle.

The radius of the $\tilde{i}^{th}$-agent-UGV's personal space at moment t_{k-1} ($t_{k-1} \in T$) equals

$$\tilde{r}_{\tilde{i}}(t_{k-1}) = \begin{cases} \hat{r}_1, \text{ if } \rho_{\tilde{i}}(t_{k-1}) = 1 \text{ and } \tilde{d}_{\tilde{i}j_b}(t_{k-1}) > l_{bu}, \\ \tilde{d}_{\tilde{i}j_b}(t_{k-1}) \text{ if } \rho_{\tilde{i}}(t_{k-1}) = 1 \text{ and } \tilde{d}_{\tilde{i}j_b}(t_{k-1}) \le l_{bu}, \\ \dfrac{\hat{r}_1}{\left(\rho_{\tilde{i}}(t_{k-1})\right)^{\eta}}, \text{ if } 1 < \rho_{\tilde{i}}(t_{k-1}) < \overline{\rho} \\ \text{and } \tilde{d}_{\tilde{i}j_b}(t_{k-1}) > l_{bu}, \\ \min\left(\tilde{d}_{\tilde{i}j_b}(t_{k-1}), \dfrac{\hat{r}_1}{\left(\rho_{\tilde{i}}(t_{k-1})\right)^{\eta}}\right), \\ \text{if } 1 < \rho_{\tilde{i}}(t_{k-1}) < \overline{\rho} \text{ and } \tilde{d}_{\tilde{i}j_b}(t_k) \le l_{bu}, \\ \hat{r}_2, \text{ if } \overline{\rho} \le \rho_{\tilde{i}}(t_{k-1}) < \overline{\overline{\rho}} \text{ and } \tilde{d}_{\tilde{i}j_b}(t_k) > l_{bu}, \\ \min\left(\tilde{d}_{\tilde{i}j_b}(t_{k-1}), \hat{r}_2\right), \text{ if } \overline{\rho} \le \rho_{\tilde{i}}(t_{k-1}) < \overline{\overline{\rho}} \\ \text{and } \tilde{d}_{\tilde{i}j_b}(t_k) \le l_{bu}, \\ 0, \text{ if } \overline{\overline{\rho}} \le \rho_{\tilde{i}}(t_{k-1}), \end{cases} \tag{3}$$

$$\tilde{i} \in I,\ b \in B,\ j_b \in J_b,\ u \in U.$$

Here, $\hat{r}_1$ is the initial value of the radius of the agent's personal space corresponding to the normal state of the density of the surrounding space (i.e. in absence of panic); $0 \leqslant \eta \leqslant 1$ is some coefficient with the fixed value ($\eta = 0.2$); $\hat{r}_2 >> \hat{r}_1$ is the value of the radius of the agent's personal space corresponding to the state of high density of the surrounding space; $\{\overline{\rho}, \overline{\overline{\rho}}\}$are the threshold values of the densities of the surrounding space; l_{bu}, $b \in B$ is the minimum required distance from the UGV to the j_{bu}^{ths}-obstacles for safe braking, taking into account the state of the road surface and illumination level $u \in U$.

The agent-UGV motion velocity depends on the radius of its personal space and presence of obstacles.

The line speed of the $\tilde{i}^{th}$-agent-UGV when driving in the linear section of the street road network at moment t_{k-1} ($t_{k-1} \in T$) is equal to

$$\tilde{v}_{\tilde{i}}(t_{k-1}) = \begin{cases} \lambda \tilde{v}_1, \text{ if } \tilde{r}_{\tilde{i}}(t_{k-1}) \in [\hat{r}_1, \hat{r}_2], \\ \lambda \psi \tilde{v}_{\tilde{i}}(t_{k-2}), \text{ if } \tilde{d}_{\tilde{i}j_b}(t_{k-1}) \le l_{bu}, \\ 0, \text{ if } \tilde{r}_{\tilde{i}}(t_{k-1}) = 0, \end{cases} \tag{4}$$

$$\tilde{i} \in I,\ b \in B,\ j_b \in J_b,\ u \in U.$$

Here, $\tilde{v}_1$ is the base velocity of UGV given through the log-normal distribution in a fixed range; $0 \leqslant \psi \leqslant 1$ is the coefficient of extreme braking ($\psi = 0.01$); λ is the coefficient that determines the ratio of the scales of real and virtual simulation time (considering the real and virtual velocities of the vehicular movement).

The angular velocity of the $\tilde{i}^{th}$-agent-UGV ($\tilde{i} \in I$) when driving in the roundabout section of the street road network at moment t_{k-1} ($t_{k-1} \in T$) is equal to

$$\tilde{v}^*_{\tilde{i}}(t_{k-1}) = \frac{\tilde{v}_{\tilde{i}}(t_{k-1})}{\tilde{d}_{\tilde{i}O}(t_{k-1})}. \tag{5}$$

Here, $\tilde{d}_{\tilde{i}O}(t_{k-1})$ is the Euclidean distance from the $\tilde{i}^{th}$-agent-UGV ($\tilde{i} \in I$) to the center of the circular motion area (see *Fig. 2a*) at moment t_{k-1} ($t_{k-1} \in T$).

The directional angle required for the angular motion of the $\tilde{i}^{th}$-agent-UGV ($\tilde{i} \in I$) located in a circular motion at moment t_{k-1} ($t_{k-1} \in T$) equals

$$\alpha_{\tilde{i}}(t_{k-1}) = \arctan\frac{y_{\tilde{i}}(t_{k-1}) - \hat{y}_O}{x_{\tilde{i}}(t_{k-1}) - \hat{x}_O} - \lambda \tilde{v}^*_{\tilde{i}}(t_{k-1}). \tag{6}$$

Here, $\{\tilde{x}_{\tilde{i}}(t_{k-1}), \tilde{y}_{\tilde{i}}(t_{k-1})\}$ are coordinates of the $\tilde{i}^{th}$-agent-UGV ($\tilde{i} \in I$) at moment t_{k-1} ($t_{k-1} \in T$); $\{\hat{x}_O, \hat{y}_O\}$ are coordinates of the center of the roundabout area.

The offset angle of the $\tilde{i}$-agent-UGV ($\tilde{i} \in I$) to bypass the nearest j_b^{th}-agent-obstacles ($j_b \in J_b$, $b \in B$) at moment t_{k-1} ($t_{k-1} \in T$) equals

$$\omega_{\tilde{i}j_b}(t_{k-1}) = \frac{\pi}{4} + \tag{7}$$

$$+\left|\arctan\frac{y_{j_b}(t_{k-1}) - \tilde{y}_{\tilde{i}}(t_{k-1}) + \left(r_{j_b}(t_{k-1}) + \tilde{r}_{\tilde{i}}(t_{k-1})\right)\sin\frac{\pi}{4}}{x_{j_b}(t_{k-1}) - \tilde{x}_{\tilde{i}}(t_{k-1}) + \left(r_{j_b}(t_{k-1}) + \tilde{r}_{\tilde{i}}(t_{k-1})\right)\cos\frac{\pi}{4}}\right|.$$

Here, $\{x_{j_b}(t_{k-1}), y_{j_b}(t_{k-1})\}$, $r_{j_b}(t_{k-1})$, are coordinates and radius of the personal space of the j_b^{th}-obstacle ($j_b \in J_b$, $b \in B$) at moment t_{k-1} ($t_{k-1} \in T$).

The angle specified the direction of movement of the $\tilde{i}^{th}$-agent-UGV ($\tilde{i} \in I$) towards the nearest neighbour (for overtaking) at moment t_{k-1} ($t_{k-1} \in T$) equals

$$\gamma^*_{\tilde{i}j_b}(t_{k-1}) = \left| \arctan \frac{y_{j_b}(t_{k-1}) - y_i(t_{k-1})}{x_{j_b}(t_{k-1}) - x_i(t_{k-1})} \right|. \quad (8)$$

The rebound angle of the $\tilde{i}^{th}$-agent-UGV ($\tilde{i} \in I$) from the nearest j_b^{th}-agent-obstacles ($j_b \in J_b$) at moment t_{k-1} ($t_{k-1} \in T$) equals

$$\gamma_{\tilde{i}j_b}(t_{k-1}) = \pi + \gamma^*_{\tilde{i}j_b}(t_{k-1}). \quad (9)$$

Here,

- $\tilde{s}_{\tilde{i}}(t_k) \in \{1, 2, 3, 4\}$ is the UGV state: $\tilde{s}_{\tilde{i}}(t_k) = 1$ is the accident state, $\tilde{s}_{\tilde{i}}(t_k) = 2$ is the initial state of the UGV at the entrance to the DRN that is saved when driving on the road linear section, $\tilde{s}_{\tilde{i}}(t_k) = 3$ is the state of the UGV movement in the roundabout area of the DRN at moment t_k ($t_k \in T$), $\tilde{s}_{\tilde{i}}(t_k) = 4$ – the state of the UGV exit from the DRN using a straight section of the road;
- $\tilde{c}_{\tilde{i}}(t_0) \in \{1, 2, 3, 4\}$ is the UGV type: $\tilde{c}_{\tilde{i}}(t_0) = 1$ is the movement from left-to-right, $\tilde{c}_{\tilde{i}}(t_0) = 2$ is the movement from right-to-left, $\tilde{c}_{\tilde{i}}(t_0) = 3$ is the movement from bottom-to-top, $\tilde{c}_{\tilde{i}}(t_0) = 4$ is the movement from top-to-bottom given at the initial moment ($t_0 \in T$).

Then, the direction of movement of the UGV in the DRN at the moment of time t_{k-1} ($t_{k-1} \in T$) can be calculated like this:

$$\tilde{w}_{\tilde{i}}(t_{k-1}) = \begin{cases} 1, \text{ if } \tilde{c}_{\tilde{i}}(t_0) \in \{1,3\} \text{ and } \tilde{s}_{\tilde{i}}(t_{k-1}) \neq 1, \\ -1, \text{ if } \tilde{c}_{\tilde{i}}(t_0) \in \{2,4\} \text{ and } \tilde{s}_{\tilde{i}}(t_{k-1}) \neq 1, \\ 0, \text{ if } \tilde{s}_{\tilde{i}}(t_{k-1}) = 0. \end{cases} \quad (10)$$

In view of the foregoing, for the considered radial-ring scheme of the digital road network, the space dynamics of the $\tilde{i}^{th}$-agent-UGV ($\tilde{i} \in \tilde{I}$) at moment t_k ($t_k \in T$) is given by the following system of the finite difference equations with the variable structure:

$$\tilde{x}_{\tilde{i}}(t_k) = \begin{cases} \tilde{x}_{\tilde{i}}(t_{k-1}) + \tilde{w}_{\tilde{i}}(t_{k-1})\lambda\tilde{v}_{\tilde{i}}((t_{k-1}), \text{ if I is true} \\ \tilde{x}_{\tilde{i}}(t_{k-1}) + \tilde{v}_{\tilde{i}}(t_k)\cos\left(\pm\tilde{\omega}_{\tilde{i}j_b}(t_{k-1})\right) + \\ + \dfrac{c_1}{d_{\tilde{i}j_b}(t_{k-1})}\cos\tilde{\gamma}_{\tilde{i}j_b}(t_{k-1}), \text{ if II is true,} \\ \tilde{x}_{\tilde{i}}(t_{k-1}) + \dfrac{c_1}{d_{\tilde{i}j_b}(t_{k-1})}\cos\tilde{\gamma}_{\tilde{i}j_b}(t_{k-1}), \\ \text{if III is true,} \\ \hat{x}_O + \tilde{d}_{\tilde{i}O}(t_{k-1})\cos\left(\lambda\tilde{v}^*_{\tilde{i}}(t_{k-1}) + \tilde{\alpha}_{\tilde{i}}(t_{k-1})\right), \\ \text{if IV is true,} \\ \left(\tilde{x}_{\tilde{i}}(t_{k-1}) + \cos\left(\begin{array}{l} \lambda\tilde{v}^*_{\tilde{i}}(t_{k-1}) + \\ \tilde{\alpha}_{\tilde{i}}(t_{k-1}) \pm \tilde{\omega}_{\tilde{i}j_b}(t_{k-1}) \end{array} \right) + \atop \dfrac{c_2}{d_{\tilde{i}j_b}(t_{k-1})}\cos\tilde{\gamma}_{\tilde{i}j_b}(t_{k-1}) \right), \\ \text{if V is true,} \\ \tilde{x}_{\tilde{i}}(t_{k-1}) + \dfrac{c_2}{d_{\tilde{i}j_b}(t_{k-1})}\cos\tilde{\gamma}_{\tilde{i}j_b}(t_{k-1}), \\ \text{if VI is true,} \\ \tilde{x}_{\tilde{i}}(t_{k-1}), \text{ if VII is true,} \end{cases} \quad (11)$$

$$\tilde{y}_{\tilde{i}}(t_k) = \begin{cases} \tilde{y}_{\tilde{i}}(t_{k-1}), \text{ if I is true,} \\ \tilde{y}_{\tilde{i}}(t_{k-1}) + \tilde{v}_{\tilde{i}}(t_k)\sin\left(\pm\tilde{\omega}_{\tilde{i}j_b}(t_{k-1})\right) + \\ + \dfrac{c_1}{d_{\tilde{i}j_b}(t_{k-1})}\sin\tilde{\gamma}_{\tilde{i}j_b}(t_{k-1}), \text{ if II is true,} \\ \tilde{y}_{\tilde{i}}(t_{k-1}) + \dfrac{c_1}{d_{\tilde{i}j_b}(t_{k-1})}\sin\tilde{\gamma}_{\tilde{i}j_b}(t_{k-1}), \\ \text{if III is true,} \\ \hat{y}_O + \tilde{d}_{\tilde{i}O}(t_{k-1})\sin\left(\lambda\tilde{v}^*_{\tilde{i}}(t_{k-1}) + \tilde{\alpha}_{\tilde{i}}(t_{k-1})\right), \\ \text{if IV is true,} \\ \left(\tilde{x}_{\tilde{i}}(t_{k-1}) + \sin\left(\begin{array}{l} \lambda\tilde{v}^*_{\tilde{i}}(t_{k-1}) + \\ \tilde{\alpha}_{\tilde{i}}(t_{k-1}) \pm \tilde{\omega}_{\tilde{i}j_b}(t_{k-1}) \end{array} \right) + \atop + \dfrac{c_2}{d_{\tilde{i}j_b}(t_{k-1})}\sin\tilde{\gamma}_{\tilde{i}j_b}(t_{k-1}) \right), \\ \text{if V is true,} \\ \tilde{x}_{\tilde{i}}(t_{k-1}) + \dfrac{c_2}{d_{\tilde{i}j_b}(t_{k-1})}\sin\tilde{\gamma}_{\tilde{i}j_b}(t_{k-1}), \\ \text{if VI is true,} \\ \tilde{y}_{\tilde{i}}(t_{k-1}) + \tilde{w}_{\tilde{i}}(t_{k-1})\lambda\tilde{v}_{\tilde{i}}(t_{k-1}), \\ \text{if VII is true,} \end{cases} \quad (12)$$

$$\tilde{i} \in I,\, b \in B,\, j_b \in J_b,$$

where

I. $s_i\,(t_{k-1}) \in \{2,\ 4\}$ and $\tilde{c}_{\tilde{i}}(t_0) \in \{1,\, 2\}$ and $\tilde{d}_{\tilde{i}j_b}(t_{k-1}) > \tilde{r}_{\tilde{i}}(t_{k-1}) + r_{j_b}(t_{k-1})$ for all $(j_b \in J_b)$, that corresponds to the conditions for the UGV movement of the in the linear section of the DRN in the direction of **left-to-right or right-to-left** (when entering or leaving the DRN) and absence of obstacles, i.e. when the distance between this UGV and other agents exceeds the sum of the lengths of the radiuses of their personal spaces;

II. $s_i(t_{k-1}) \in \{2, 4\}$ and $\tilde{d}_{\tilde{i}j_b}(t_{k-1}) \le \tilde{r}_{\tilde{i}}(t_{k-1}) + r_{j_b}(t_{k-1})$ for the nearest $(j_b \in J_b)$ and $\gamma^*_{\tilde{i}j_b}(t_{k-1}) = 0$, that corresponds to the conditions of the UGV movement in the linear section of the DRN (in any direction) and **presence (appearance) of an obstacle** located ahead of the given UGV (i.e., occupying the same lane at a critically close distance), which causes manoeuvering in the form of overtaking or bypassing this obstacle;

III. $s_i(t_{k-1}) \in \{2, 4\}$ and $\tilde{d}_{\tilde{i}j_b}(t_{k-1}) \le \tilde{r}_{\tilde{i}}(t_{k-1}) + r_{j_b}(t_{k-1})$ for the nearest $(j_b \in J_b)$ and $\gamma^*_{\tilde{i}j_b}(t_{k-1}) > 0$, that corresponds to the conditions for the vehicular movement on the linear section of the CPC (in any direction) and **presence of an obstacle** that is not ahead of this vehicle (i.e., located behind or on the side at a critically close distance), which causes manoeuvering in the form of increasing the distance relative to this obstacle (i.e. accelerating, braking or avoiding a collision);

IV. $s_i(t_{k-1}) = 3$ and $\tilde{d}_{\tilde{i}j_b}(t_{k-1}) \le \tilde{r}_{\tilde{i}}(t_{k-1}) + r_{j_b}(t_{k-1})$ for all $(j_b \in J_b)$, that corresponds to the conditions for the UGV movement **in the circular motion area** of the DRN and absence of obstacles;

V. $s_i\,(t_{k-1}) = 3$ and $\tilde{d}_{\tilde{i}j_b}(t_{k-1}) \le \tilde{r}_{\tilde{i}}(t_{k-1}) + r_{j_b}(t_{k-1})$ for the nearest $(j_b \in J_b)$ and $\gamma^*_{\tilde{i}j_b}(t_{k-1}) > 0$, that corresponds to the conditions for the vehicle movement in the circular motion area of the DRN and **presence (appearance) of an obstacle** located in front of this vehicle, which causes manoeuvering in the form of overtaking or bypassing this obstacle;

VI. $s_i(t_{k-1}) = 3$ and $\tilde{d}_{\tilde{i}j_b}(t_{k-1}) \le \tilde{r}_{\tilde{i}}(t_{k-1}) + r_{j_b}(t_{k-1})$ for the nearest $(j_b \in J_b)$ and $\gamma^*_{\tilde{i}j_b}(t_{k-1}) > 0$, that corresponds to the conditions for the vehicular movement in the circular motion area of the DRN and presence of an obstacle that is **not in front of this vehicle**, which necessitates manoeuvering in the form of increasing the distance relative to this obstacle;

VII. $s_i(t_{k-1}) \in \{2, 4\}$ and $\tilde{c}_{\tilde{i}}(t_0) \in \{3, 4\}$ and $\tilde{d}_{\tilde{i}j_b}(t_{k-1}) > \\ > \tilde{r}_{\tilde{i}}(t_{k-1}) + r_{j_b}(t_{k-1})$ for all $(j_b \in J_b)$itions for the UGV movement in the linear section of the DRN in the direction of **bottom-up or top-down** (when entering or leaving the DRN) and no obstacles.

Next, the software implementation of the proposed model (11)–(12) using FLAME GPU will be presented.

2. Software implementation

The software implementation of the traffic model of interacting UGVs with other road users allows us to study the rate of road accidents under various configurations of the digital road network (DRN) (*Fig. 4*).

The choice of the best street road network configuration should be based on a combination of computational and expert decision-making methods. The use of the simulation model we developed makes it possible to form a set of trade-offs for the implementation of the intelligent transportation system of the 'smart city' and its modes of operation. At the same time, genetic optimization algorithms [2, 3], scenario analysis methods [4, 5], etc., can be used to improve the values of the objective functions of the system: the total output traffic and the number of potential accidents. Further, based on the methods of expert assessment [26, 27], practical recommendations can be obtained on the transformation of the configuration of the DRN and using UGVs with characteristics that provide the required safety level of the 'smart city.'

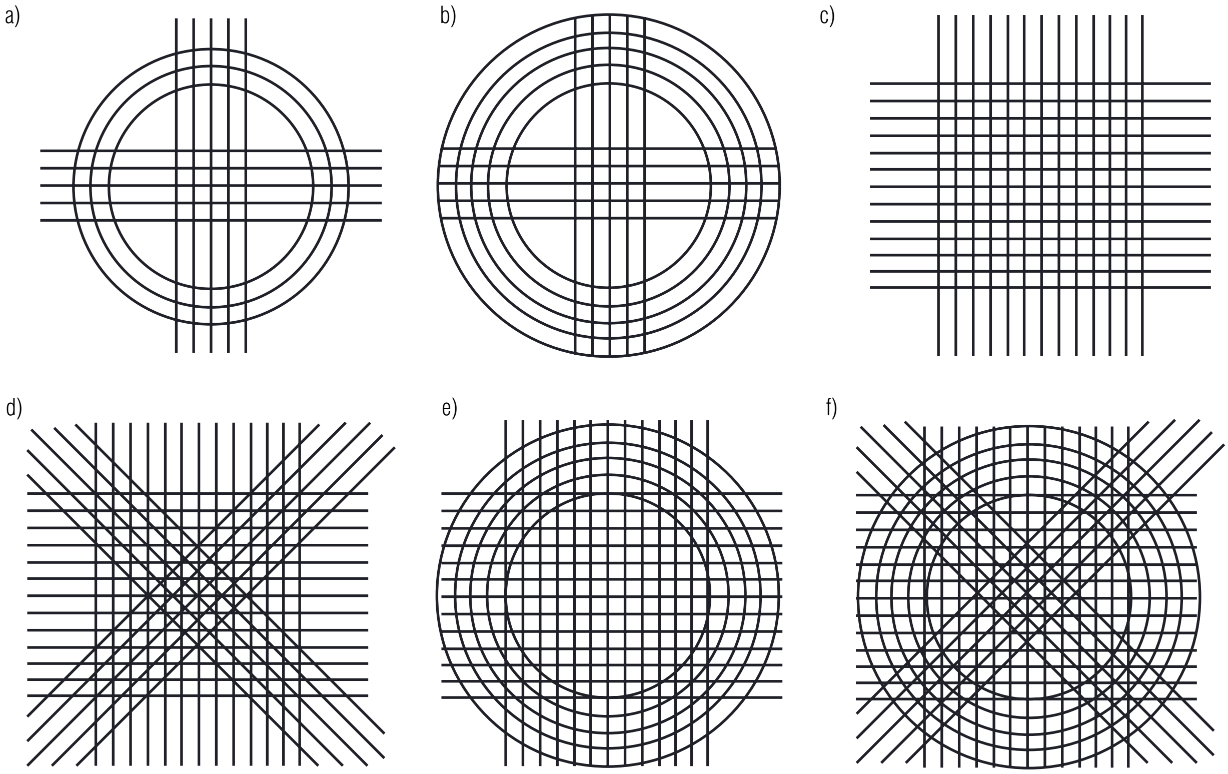

Fig. 4. DRN configurations: a) simple radial–annular, b) extended radial–circular, c) rectangular, d) rectangular–diagonal, e) rectangular–circular, f) rectangular–diagonal–circular.

The software implementation of such a model was made using the FLAME GPU framework (https://flamegpu.com/) that provides efficient parallelization of the behavior logic of interacting agents and their individual decision-making systems.

Table 1 provides a description of the functions developed in C++ using the FLAME GPU.

Table 1 contains mainly two types of functions: FLAMEGPU_STEP_FUNCTION and FLAMEGPU_AGENT_FUNCTION. Functions of the first type are executed at each moment of simulation time at the level of the central processing unit (CPU), and functions of the second type are executed in parallel computing mode using graphics processing units (GPUs). Thus, the logic of each agent behavior is parallelized (including control if the velocity, manoeuvering, etc.). As a result, the simulation model we developed makes it possible to investigate the behavior of an ensemble of UGVs, MGVs, and other agents in the scale of the 'smart city' (i.e., to simulate traffic that includes tens and hundreds of thousands of interacting road users). The visualization of the spacial dynamics of agents is carried out using the **OpenGL** that is a special application programming interface (API) providing the ability to draw multiple objects, both stationary and mobile (*Fig. 5*).

As a result, it is possible to visualize the spacial distribution of agents in the DRN and assess the composition and state of road users (UGVs, MGVs, vehicles in the accident state, etc.), which significantly simplifies the validation process for the model developed.

Table 1.

Basic computational procedures and functions of the traffic simulation model

Function name	Appointment	Input messages	Output messages
FLAMEGPU_INIT_FUNCTION (init_function)	Model initialization. Formation of the configuration of the DRN in accordance with the specified value of the control parameter of the model. Generation of the initial population of agents (UGVs and MGVs).	No	No
FLAMEGPU_STEP_FUNCTION (basic output)	Generation of new agents (UGVs and MGVs) and their arriving to the DRN with a given intensity. Formation of agents–obstacles (for example, pedestrians) in the road sections of the DRN.	No	No
FLAMEGPU_STEP_FUNCTION (agents_data_updating)	Implementation of the hierarchical clustering algo–rithm to identify problem areas of the DRN to UGVs can bypass the emerging traffic jams. Saving data on the spacial location of agents and their characteristics for the further visualization using the OpenGL.	No	No
FLAMEGPU_AGENT_FUNCTION (density_estimation, flamegpu::MessageSpatial2D, flamegpu::MessageNone)	Assessment of the traffic density around the agent–vehicle, changing the radius of the agent's personal space and its speed when interacting with other agents (e.g., reducing the radius of the agent's personal space in high–density traffic and increasing it when there are obstacles). Computing the direction angle and distance to the nearest agent for the purpose of the further manoeuvering (overtaking or braking). Monitoring emergency situations (accidents).	Agent Data	No
FLAMEGPU_AGENT_FUNCTION (update_agent_state, flamegpu::MessageNone, flamegpu::MessageSpatial2D)	Calculation of the resulting characteristics of the model (e.g., the total number of accidents, output traffic). Transfer of data about the agent–vehicle to other road users.	No	Agent Data
FLAMEGPU_AGENT_FUNCTION (agent_move, flamegpu::MessageNone, flamegpu::MessageNone)	Spacial movement of the agent in the DRN in accordance with the given rules of individual decision– making, e.g. entry (or exit) into (or outside) the DRN at the rectilinear movement, roundabout, manoeuvering, etc.	No	No
void display()	Visualization of the DRN and spacial dynamics of agents using the OpenGL at each moment of simulation time.	No	No

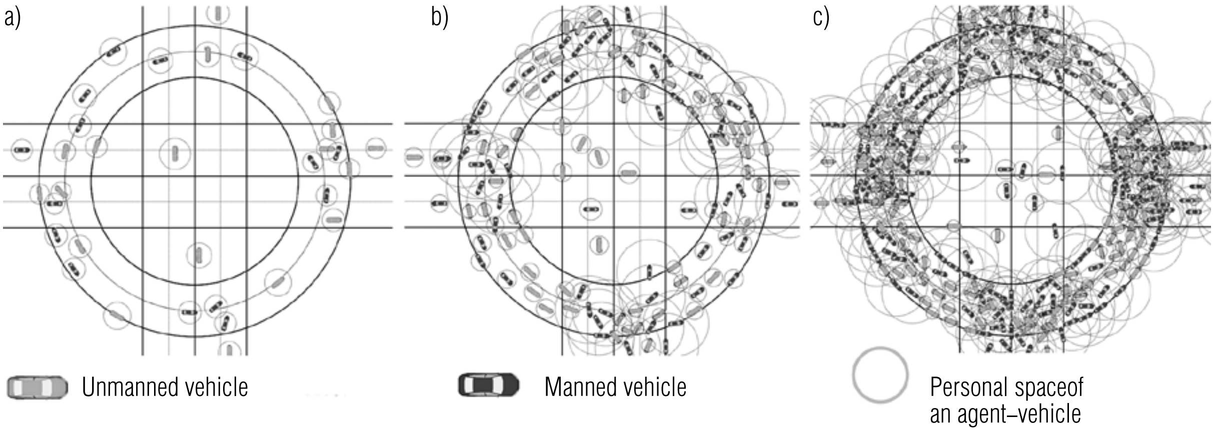

Fig. 5. Spacial dynamics of agents in a simple radial–annular DRN:
a) low–intensity traffic, b) medium–intensive traffic, c) high–intensity traffic.

3. Results of numerical experiments

Table 2 presents the resulting characteristics of the simulation model: the total output traffic (TOT) and number of vehicles in the accident state (VAS), calculated for the final time point (60 min.) under various scenarios and in absence of extreme situations, i.e. in conditions of sufficient visibility, with a dry road surface, absence of unexpected obstacles in the form of pedestrians, etc.:

- **Scenario 1.** *Low-intensity and low-speed movement of UGVs.* The vase velocity of UGVs and MGVs equals to 45–65 km/h, the intensity of vehicles arrival to the DRN is 1 vehicle every 10 sec.
- **Scenario 2.** *Medium-intensive and medium-speed movement of UGVs.* The vase velocity of UGVs and MGVs equals to 65–90 km/h, the intensity of vehicles arrival in the DRN is 5 vehicles every 10 sec.

Table 2.

Outbound traffic and number of potential accidents in absence of emergencies

DRN configurations	Scenario 1		Scenario 2		Scenario 3	
	TOT (traffic)	VAS (accidents)	TOT (traffic)	VAS (accidents)	TOT (traffic)	VAS (accidents)
Simple radial–annular	706	0	905	2	2810	6
Expanded radial–annular	851	0	1321	2	3100	6
Rectangular	1010	0	1532	2	3520	8
Rectangular–diagonal	1205	0	1720	2	3610	8
Rectangular–ring	1305	0	1850	2	3750	10
Rectangular–diagonal–ring	1530	0	2120	2	4111	12

- **Scenario 3.** *High-intensity and high-speed movement of UGVs.* The base speed of UGVs and MGVs: 100–120 km/h, intensity of vehicle arrival to the DRN is 10 vehicles every 10 sec.

Table 3 presents the resulting characteristics of the simulation model in the presence of extreme conditions (i.e., in conditions of insufficient visibility, wet road surface, unexpected appearance of pedestrians, cyclists and other obstacles on the roadway, etc.).

Figure 6 shows the rate of traffic accidents (cumulatively) for the Scenario 3 (*Table 3*), i.e. in high-intensity and high-speed movement of UGVs in extreme situations. At the same time, *Fig. 6* shows the quantitative characteristics of traffic congestion caused by the effects of the 'turbulence' and 'crash' that described in [6, 17], earlier.

As shown in *Fig. 6*, the rate of road accidents (i.e. the number of vehicles in the accident state) is associated with an increase in the number and average density of traffic congestion. Thus, the growth in the total number and scale of traffic jams in the DRN under conditions of high-intensity and high-speed traffic is the most important factor causing accidents, including those involving the UGV, which periodically have collisions with unexpected obstacles. A similar phenomenon is explained by attempts to manoeuvre (e.g., extreme braking, overtaking, etc.) from the side of vehicles, which, in conditions of traffic congestion, often leads to accidents. However, as follows from *Table 3*, a reduction in the velocity limit (up to 45–65 km/h) and the density of vehicles arriving at the DRN (up to 0.1 vehicles per second) ensures the high level of road safety even in extreme situations.

Conclusion

The article presents an approach to simulation of the road traffic accident rates with the participation of unmanned ground vehicles within a multi-agent intelligent transportation system of the 'smart city' (*Fig. 1*). We suggest a model of the UGVs ensemble movement in the digital road network (DRN) with the implementation on the example of a simple radial-ring scheme of the street road network (*Fig. 3*). Such a model, using a system of finite-difference equations with variable structure (11)–(12), makes it possible to study the

Table 3.

Outbound traffic and number of potential accidents in extreme situations

DRN configurations	Scenario 1		Scenario 2		Scenario 3	
	TOT (traffic)	VAS (accidents)	TOT (traffic)	VAS (accidents)	TOT (traffic)	VAS (accidents)
Simple radial–annular	655	2	870	2	2800	12
Expanded radial–annular	760	2	1210	4	3100	14
Rectangular	980	0	1310	6	3462	14
Rectangular–diagonal	1110	0	1622	8	3423	16
Rectangular–ring	1210	2	1780	8	3554	18
Rectangular–diagonal–ring	1400	2	2100	10	3780	20

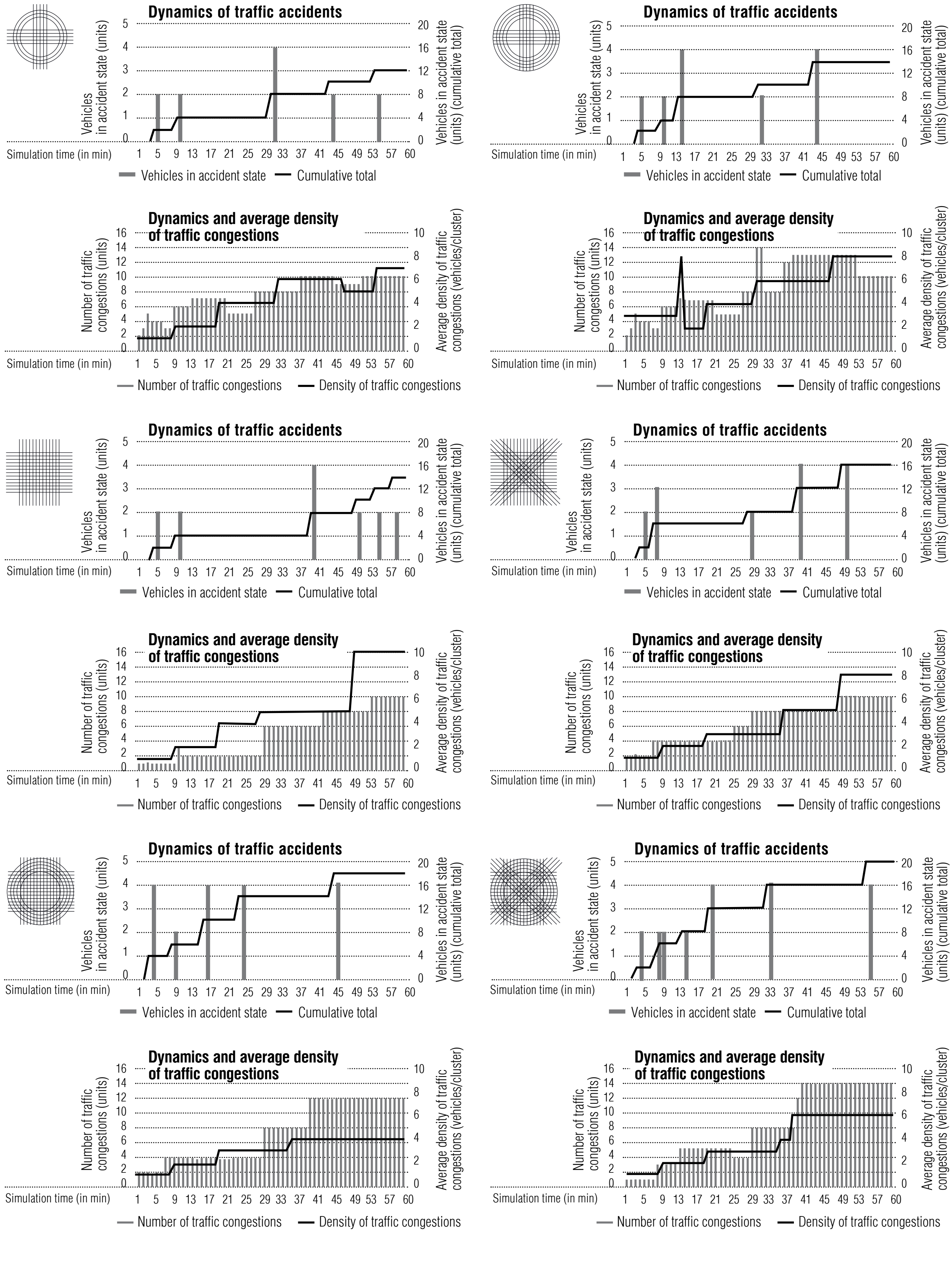

Fig. 6. Dynamics of accidents and characteristics of traffic congestions under different configurations of the digital road network (DRN): the occurrence of new accidents is interconnected with the appearance of traffic jams and an increase in their average density and depends on the DRN's geometry.

spacial dynamics of agent-UGVs interaction with various obstacles as MGVs, unexpectedly emerging pedestrians, etc. for various configurations of the DRN (*Fig. 4*). At the same time, each agent-UGV has an individual decision-making system for manoeuvering aimed at preventing emergency situations, in particular, by changing the radius of the personal space of the agent-UGV, reducing speed, bypassing unexpected obstacles, etc. (*Fig. 2*). The proposed simulation model was implemented using the large-scale agent-based simulation framework FLAME GPU, which made it possible to study the behavior of the UGVs ensemble interaction with other agents, including under high traffic conditions (*Fig. 5*). The numerical results (*Fig. 6*, *Tables 2–3*) so obtained confirm the possibility of achieving the required level of road safety even in extreme situations.

Further research will be aimed at solving the problems of optimal routing of UGVs within the DRN to minimize the impact of traffic congestion and forced manoeuvering on the accident rates. ■

Acknowledgments

The reported study was funded by RFBR, project number 19-29-06003.

References

1. Makarov V.L., Bakhtizin A.R., Beklaryan G.L., Akopov A.S. (2019) Simulation modelling of the smart city system: Concept, methods and cases. *National Interests: Priorities and Security*, vol. 15, no. 2 (371), pp. 200–224 (in Russian). https://doi.org/10.24891/ni.15.2.200
2. Akopov A.S., Beklaryan L.A., Thakur M. (2022) Improvement of maneuverability within a multiagent fuzzy transportation system with the use of parallel biobjective real-coded genetic algorithm. *IEEE Transactions on Intelligent Transportation Systems*, vol. 23, no. 8, pp. 12648–12664. https://doi.org/10.1109/TITS.2021.3115827
3. Akopov A.S., Beklaryan L.A., Beklaryan L.A. (2021) Simulation-based optimization for autonomous transportation systems using a parallel real-coded genetic algorithm with scalable nonuniform mutation. *Cybernetics and Information Technologies*, vol. 21, no. 3, pp. 127–144. https://10.2478/cait-2021-0034
4. Akopov A.S., Beklaryan A.L. (2021) Scenario simulation of autonomous vehicles motion in artificial road network using FLAME GPU. *Artificial societies*, vol. 16, no. 1 (in Russian). https://doi.org/10.18254/S207751800014028-9
5. Akopov A.S., Beklaryan L.A., Beklaryan A.L., Belousov F.A. (2021) Simulation of motion of an ensemble of unmanned ground vehicles using FLAME GPU. *Informacionnye Tehnologii*, vol. 27, no. 7, pp. 369–379 (in Russian). https://doi.org/10.17587/it.27.369-379
6. Akopov A.S., Beklaryan L.A., Khachatryan N.K., Beklaryan A.L., Kuznetsova E.V. (2020) Multi-agent control system for unmanned ground vehicles. I*nformacionnye Tehnologii,* vol. 26, no. 6, pp. 342–353 (in Russian). https://doi.org/10.17587/it.26.342-353
7. Andreev K.P., Kildishev A.A., Terentiev V.V., Shemiakin A.V. (2019) Safety assessment of transport units by means of computer simulation. *Byulleten' transportnoj informacii,* no. 1 (283), pp. 20–23 (in Russian).
8. Kolotov V.V., Kolyuzhnov V.V. (2011) Intelligent transport system and road situation modelling. *Vestnik komp'yuternyh i informacionnyh tekhnologij,* no. 12 (90), pp. 53–56 (in Russian).
9. Astarita V., Pasquale Giofré V. (2019) From traffic conflict simulation to traffic crash simulation: Introducing traffic safety indicators based on the explicit simulation of potential driver errors. S*imulation Modeling Practice and Theory*, vol. 94, pp. 215–236. https://doi.org/10.1016/j.simpat.2019.03.003
10. Kravchenko T.K., Isaev D.V. *Decision support systems.* Moscow: Urait, 2017 (in Russian).

11. Brännström M., Coelingh E., Sjöberg J. (2010) Model-based threat assessment for avoiding arbitrary vehicle collisions. I*EEE Transactions on Intelligent Transportation Systems*, vol. 11, no. 3, pp. 658–669. https://doi.org/10.1109/TITS.2010.2048314
12. Cheng S., Li L., Guo H.-Q., Chen Z.-G., Song P. (2020) Longitudinal collision avoidance and lateral stability adaptive control system based on MPC of autonomous vehicles. *IEEE Transactions on Intelligent Transportation Systems,* vol. 21, no. 6, pp. 2376–2385. https://doi.org/10.1109/TITS.2019.2918176
13. Petrović D., Mijailović R., Pešić D. (2020) Traffic accidents with autonomous vehicles: Type of collisions, manoeuvres and errors of conventional vehicles' drivers. T*ransportation Research Procedia,* vol. 45, pp.161-168. https://doi.org/10.1016/j.trpro.2020.03.003
14. Wang H., Huang Y., Khajepour A., Zhang Y., Rasekhipour Y., Cao D. (2019) Crash mitigation in motion planning for autonomous vehicles. *IEEE Transactions on Intelligent Transportation Systems*, vol. 20, no. 9, pp. 3313–3323. https://doi.org/10.1109/TITS.2018.2873921
15. Wang J., Wu J., Li Y. (2015) The driving safety field based on driver–vehicle–road interactions. *IEEE Transactions on Intelligent Transportation Systems*, vol. 16, no. 4, pp. 2203–2214. https://doi.org/10.1109/TITS.2015.2401837
16. You F., Zhang R., Lie G., Wang H., Wen H., Xu J. (2015) Trajectory planning and tracking control for autonomous lane change maneuver based on the cooperative vehicle infrastructure system. *Expert Systems with Applications*, vol. 42, no. 14, pp. 5932–5946. https://doi.org/10.1016/j.eswa.2015.03.022
17. Akopov A.S., Beklaryan L.A. (2015) An agent model of crowd behaviour in emergencies. *Automation and Remote Control*, vol. 76, no. 10, pp. 1817–1827. https://doi.org/10.1134/S0005117915100094
18. Richmond P., Walker D., Coakley S., Romano D. (2010) High performance cellular level agent-based simulation with FLAME for the GPU. *Briefings in Bioinformatics*, vol. 11, no. 3, pp. 334–347. https://doi.org/10.1093/bib/bbp073
19. Heywood P., Richmond P., Maddock S. (2015) Road network simulation using FLAME GPU. In: *Euro-Par 2015: Parallel-Processing Workshops. Lecture Notes in Computer Science*, vol. 9523. Springer, Cham, pp. 430–431. https://doi.org/10.1007/978-3-319-27308-2_35
20. Helbing D. (2001) Traffic and related self-driven many-particle systems // *Reviews Of Modern Physics*, vol. 73, no. 4, pp. 1067–1141. https://doi.org/10.1103/RevModPhys.73.1067
21. Helbing D., Buzna L., Johansson A., Werner T. (2005) Self-organized pedestrian crowd dynamics: Experiments, simulations, and design solutions. *Transportation Science*, vol. 39, no. 1, pp. 1–24. https://doi.org/10.1287/trsc.1040.0108
22. Khachatryan N.K., Akopov A.S. (2017) Model for organizing cargo transportation with an initial station of departure and a final station of cargo distribution. *Business Informatics*, vol. 1, no. 39, pp. 25–35. https://doi.org/10.17323/1998-0663.2017.1.25.35
23. Belousov F.A., Khachatryan N.K., Nevolin I.V. (2022) Reduction of dimension in the problem of optimal management of a freight cars fleet using unmanned locomotives. *Business Informatics*, vol. 2, no. 16, pp. 7-20. https://doi.org/10.17323/2587-814X.2022.2.7.20
24. Mullner D. (2013) fastcluster: Fast hierarchical, agglomerative clustering routines for R and Python. *Journal of Statistical Software*, 53, no. 9, pp. 1–18. https://doi.org/10.18637/jss.v053.i09
25. Kostsov A.V., Bakhirev I.A., Borovik E.N., Martyakhin D.S. (2017) *Transport planning of cities. Textbook*. Moscow: A-project (in Russian).
26. Kravchenko T.K., Isaev D.V. (2016) Making strategic decisions under risk and uncertainties. *Finance: Theory and Practice*, vol. 20, no. 4, pp. 22–31 (in Russian). https://doi.org/10.26794/2587-5671-2016-20-4-22-31
27. Isaev D.V. (2022) Making strategic management decisions based on a combination of computation and expert methods. *Proceedings of the XXIII All-Russian Symposium "Strategic Planning and Development of Enterprises"*, Moscow: CEMI RAS, pp. 174–176 (in Russian). https://doi.org/10.34706/978-5-8211-0802-9-s2-10

About the authors

Andranik S. Akopov

Dr. Sci. (Tech.), Professor; Professor of the Russian Academy of Sciences;

Chief Researcher, Laboratory of Dynamic Models of Economy and Optimization, Central Economics and Mathematics Institute, Russian Academy of Sciences, 47, Nachimovky Prospect, Moscow 117418, Russia;

E-mail: akopovas@umail.ru

ORCID: 0000-0003-0627-3037

Levon A. Beklaryan

Dr. Sci. (Phys.-Math.), Professor;

Chief Researcher, Laboratory of Dynamic Models of Economy and Optimization, Central Economics and Mathematics Institute, Russian Academy of Sciences, 47, Nakhimovsky Prospect, Moscow 117418, Russia;

E-mail: beklar@cemi.rssi.ru

ORCID: 0000-0001-5695-4450